ENGINEERING MECHANICS 2009
National Conference with International Participation
Svratka, Czech Republic, May 11 – 14, 2009

pp. 1143–1158
Paper **#259**

MOTION SIMULATION OF A RAILWAY VEHICLE BOGIE ALONG DIRECT WAVED RAILWAY

J. Siegl*, J. Švígler*

Summary: *This paper is devoted to the dynamical analysis of a vehicle bogie motion along a direct waved railway. A mathematical model of the discrete multibody system that consists of one half vehicle case and a bogie with double suspension is created. The exact time change of a wheel-rail contact point position during vehicle motion, when a wheel carries out a general spatial motion, is included into the solution. The rails and vehicle wheels are interconnected through the creep force effects. Numerical solution and graphical visualization of the vehicle bogie motion with the constant vehicle forward velocity, with consideration of variable creep force effects, is performed. The results are compared with vehicle bogie motion along the direct not waved railway and an influence of railway waviness to the vehicle bogie motion stability is shown.*

1. Introduction

The railway vehicle is considered as a closed kinematical chain that creates a multibody system with 22 degrees of freedom. Each body of this system is considered perfectly rigid with immaterial link elements. The railway, which is considered infinitely material, is connected to the vehicle wheels by creep elements. Vehicle bogie primary and secondary suspension is modeled by spring and damper elements. The rail head profile is modeled exactly in accordance with the profile UIC 60 and the rails waviness in the vertical longitudinal plane has a form of harmonic function. The following assumptions are considered for motion equations developing of the vehicle bogie system. The wheel sets run freely in the journal bearings without bearing friction and do not generate either tractive or braking force effects. Displacements in suspension elements are considered great. The wheel-flange contact and nonlinearities in adhesion limits between wheel and rail are neglected. The sim-

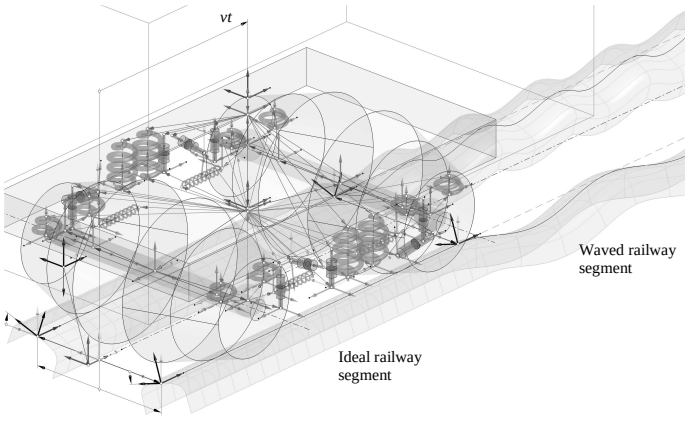

Fig. 1 Geometrical visualisation of the dynamic model of the railway vehicle bogie.

* Ing. Jaroslav Siegl, Doc. Ing. Jaromír Švígler, CSc.: University of West Bohemia, Faculty of Applied Sciences, Department of Mechanics; Univerzitní 22; 30100 Pilsen; e-mail: jsiegl@kme.zcu.cz, svigler@kme.zcu.cz; tel.: +420 377 632 381, +420 377 632 304;

plified wheel contact geometry and the linear creep theory is used. The gyroscope moments of wheel sets are neglected. There is no wheel lift and the wheels are always in contact with the rails.

2. Nomenclature

A generalized coordinate in the 3-dimensional space of a space *b* expressed in a space *a* is written by the vector

$$ {}^{a}\mathbf{q}_b = \left[{}^{a}\mathbf{r}_b^{\,T} \quad {}^{a}\boldsymbol{\varphi}_b^{\,T} \right]^T = \left[{}^{a}r_b^{\,1} \quad {}^{a}r_b^{\,2} \quad {}^{a}r_b^{\,3} \quad 1 \;\middle|\; {}^{a}\varphi_b^{\,1} \quad {}^{a}\varphi_b^{\,2} \quad {}^{a}\varphi_b^{\,3} \quad 0 \right]^T \in \mathbb{R}^8 \tag{1} $$

where ${}^{a}\mathbf{r}_b$, ${}^{a}\boldsymbol{\varphi}_b \in \mathbb{R}^4$ is a linear and an angular coordinate vector of the space *b* in the space *a*. The *i*-th angular coordinate determines rotation arround the *i*-th base vector $\mathbf{e}_{ia}$, sometimes called *roll*, *pitch* and *yaw* angles. The left upper index means generaly a name of a space in which a given quantity is expressed. A transformation matrix ${}^{a}\mathbf{T}_b \in \mathbb{R}^{4\times4}$ determines a space *b* expressed in a space *a*. This matrix of a 3-dimensional space has structure

$$ {}^{a}\mathbf{T}_b = \left[{}^{a}\mathbf{e}_{1b} \quad \cdots \quad {}^{a}\mathbf{e}_{3b} \quad {}^{a}\mathbf{r}_b \right] \tag{2} $$

where ${}^{a}\mathbf{r}_b \in \mathbb{R}^4$ is a space position or origin and ${}^{a}\mathbf{e}_{ib} \in \mathbb{R}^4$ is the *i*-th *space generator*, ergo any set of 3-linearly independent vectors capable of generating 3-dimensional vector space. The work uses right-handed Cartesian coordinate systems whose the first base vectors are marked by black dots at the vertex of a vector conus on all figures. A transformation matrix (upper-case letter π)

$$ {}^{a}\boldsymbol{\Pi}_b = \left[\begin{array}{c|c} {}^{a}\mathbf{T}_b & \mathbf{0}_{4\times4} \\ \hline {}^{a}\mathbf{R}_b\,{}^{a}\mathbf{T}_b & {}^{a}\mathbf{T}_b \end{array} \right] \in \mathbb{R}^{8\times8} \tag{3} $$

equivalently replaces a force effect vector from the space *b* in the space *a*, where the matrix ${}^{a}\mathbf{R}_b = \mathrm{v2m}\left({}^{a}\mathbf{r}_b\right) \in \mathbb{R}^{4\times4}$ is a position vector in the matrix form of the space origin *b* expressed in the space *a* and v2m function constructs prosition vector in the matrix form.

3. Multibody dynamics

The railway vehicle is understood as a multibody system. Each body is modelled as a point mass. The list of original bodies is shown in the Tab. 1, however, a ballast and a sleeper are not considered in this model yet. The *j*-th copy of the *i*-th body are marked *ij* and the unique identifying number of this body *ij* is marked *m*, see Tab. 2. The bodies of this multibody system are connected by link elements.

Part *i*	Name of body
1	Case of vehicle
2	Frame of bogie
3	Axle shaft
4	Axle box left
5	Axle box right
6	Wheel
10	Rail
11	Sleeper
12	Ballast
13	Earth

Tab. 1 List of parts

4. Model structural elements

All link element types are considered immaterial.

4.1. Mass element

The *m*-th body of a system is modeled as a mass point. A force effect affects this mass element at the time *t* in the actual space *m*

$$\begin{aligned} {}^{m}\mathbf{Q}_{m}(t) &= {}^{m}\mathbf{Q}_{m}\left({}^{m0}\ddot{\mathbf{q}}_{m}, {}^{m0}\dot{\mathbf{q}}_{m}, {}^{r0}\dot{\mathbf{q}}_{r}, {}^{m0}\mathbf{q}_{m}, {}^{r0}\mathbf{q}_{r}\right), \\ {}^{m}\mathbf{Q}_{m}(t) &= {}^{m}\mathbf{Q}_{Im} + {}^{m}\mathbf{Q}_{Em} + {}^{m}\mathbf{Q}_{Gm} \end{aligned} \tag{4}$$

where ${}^{m}\mathbf{Q}_{Im}, {}^{m}\mathbf{Q}_{Em}, {}^{m}\mathbf{Q}_{Gm}$ is inertia, link elements and gravity force effect, respectively, *r* is a body number that is linked with the *m*-th body by link elements.

4.1.1. Inertia force effect

The inertia force effect is linearly dependent on the *m*-th body acceleration

$${}^{m}\mathbf{Q}_{Im}\left({}^{m0}\ddot{\mathbf{q}}_{m}\right) = -{}^{m}\mathbf{M}_{m}\,{}^{m0}\ddot{\mathbf{q}}_{m}, \qquad {}^{m}\mathbf{M}_{m} = \left[\begin{array}{cc|c} m_{m}\mathbf{E}_{3\times3} & \mathbf{0}_{3\times1} & \mathbf{0}_{4\times4} \\ \mathbf{0}_{1\times3} & 0 & \\ \hline & & {}^{m}\mathbf{I}_{m} \;\; \mathbf{0}_{3\times1} \\ \multicolumn{2}{c|}{sym} & \mathbf{0}_{1\times3} \;\; 0 \end{array}\right] = const \tag{5}$$

where ${}^{m}\mathbf{M}_{m} \in \mathbb{R}^{8\times8}$ is a constant *mass matrix* of the *m*-th body expressed in the actual body space *m* which is placed in the *principal central axes of inertia* of this body, $m_{m} \in \mathbb{R}^{1}$ a mass, $\mathbf{E}$ the identity matrix and ${}^{m}\mathbf{I}_{m} \in \mathbb{R}^{3\times3}$ a mass inertia tensor or body rotational mass inertia.

4.1.2. Link elements force effect

If the *m*-th body is connected to the *r*-th and the *s*-th body then the total force effect affecting the *m*-th body is described

$${}^{m}\mathbf{Q}_{Em}\left({}^{r0}\mathbf{q}_{r}, {}^{m0}\mathbf{q}_{m}, {}^{s0}\mathbf{q}_{s}\right) = {}^{m}\mathbf{Q}_{EmA} + {}^{m}\mathbf{Q}_{ErB} \tag{6}$$

where ${}^{m}\mathbf{Q}_{EmA}$ is a force effect caused by relative motion between *m*-th and *s*-th body, hence this force effect affects at the start point *A* of the actual link element placed in the *m*-th body. The force effect ${}^{m}\mathbf{Q}_{ErB}$ is caused by a relative motion between *r*-th and *m*-th body, hence this force effect affects at the end point *B* of link element placed in the *r*-th body. The total link elements force effect ${}^{m}\mathbf{Q}_{EmX}$ is given by the equivalent replacement of each *l*-th link element force effect

$${}^{m}\mathbf{Q}_{EmX}^{EType} = \sum_{l=1}^{l_{n}}\left({}^{m}\mathbf{\Pi}_{EmlX}\,{}^{EmlX}\mathbf{Q}\right) \tag{7}$$

where *EType* can be *S*, *J*, *D*, *C* for spring, joint, damper and contact creep element respectively, *X* can be *A* or *B* for the link element begin or end point, l_n is *EType* link elements number.

4.1.3. Gravitational force effect

The action gravitational force effect on the *m*-th body caused by the Earth gravitational field about generalized acceleration ${}^{g}\ddot{\mathbf{q}}_{G} = \begin{bmatrix} 0 & 0 & -g & 0 & 0 & 0 & 0 & 0 \end{bmatrix}^{T}$ expressed in the global space *g* is

$${}^{m}\mathbf{Q}_{Gm} = {}^{m}\mathbf{M}_{m}\,{}^{m}\ddot{\mathbf{q}}_{G} \tag{8}$$

where g is gravitational acceleration, ${}^{m}\ddot{\mathbf{r}}_{G} = {}^{m}\mathbf{T}_{g}\,{}^{g}\ddot{\mathbf{r}}_{G}$, ${}^{m}\mathbf{T}_{g} = \mathrm{inv}\left({}^{g}\mathbf{T}_{m}\right)$, ${}^{g}\mathbf{T}_{m} = {}^{g}\mathbf{T}_{10}\,{}^{10}\mathbf{T}_{m0}\,{}^{m0}\mathbf{T}_{m}$. The moving space of the case equilibrium state 10 is described

$$ {}^{g}\mathbf{T}_{10}(t) = {}^{g}\mathbf{T}_{D1}\underbrace{{}^{D1}\mathbf{T}_{C1k}\left(t_1\left(u_{4j}{}^{1}\right)\right)}_{\text{Railway center line}}\mathbf{T}_{3}\left(q_{10}{}^{3}\right) \tag{9} $$

where curvilinear coordinate on the railway $u_{4j}{}^{1} = u_{4j}{}^{1}(vt)$ and v is a forward velocity.

4.2. Spring element

A spring element is an oscillation insulator with almoust 100% energy accumulation. The l-th spring element causes a react force effect between the a-th and the b-th body

$$ {}^{\bar{a}}\mathbf{Q}_{A}\left({}^{a0}\mathbf{q}_{a},\ {}^{b0}\mathbf{q}_{b}\right) = \begin{bmatrix} {}^{\bar{a}}\mathbf{F}_{A}\left({}^{a0}\mathbf{q}_{a},\ {}^{b0}\mathbf{q}_{b}\right) \\ \mathbf{0}_{4\times 1} \end{bmatrix}, \tag{10} $$

$$ {}^{\bar{a}}\mathbf{F}_{A} = {}^{\bar{a}}\mathbf{T}_{EalA}\,{}^{EalA}\mathbf{F}_{A} = {}^{\bar{a}}\mathbf{T}_{EalA}\underbrace{\begin{bmatrix} 1 & 0 & & 0 \\ 0 & 1 & \dfrac{{}^{EalA}\mathbf{v}}{\left\|{}^{EalA}\mathbf{v}\right\|} & 0 \\ 0 & 0 & & 0 \\ 0 & 0 & & 1 \end{bmatrix}}_{{}^{EalA}\mathbf{T}_{S}}\begin{bmatrix} Q_1\left({}^{S}d^{1}\right) \\ Q_1\left({}^{S}d^{2}\right) \\ Q_3\left({}^{S}d^{3}\right) \\ 0 \end{bmatrix} \tag{11} $$

where $\mathbf{v}$ is a vector in the spring axis from the spring start point A to the end point B and $\mathbf{d}$ is a spring displacement vector in the special space S. This vector is assembled

$$ {}^{S}\mathbf{d} = \begin{bmatrix} {}^{EalA}v_{a}{}^{1} & {}^{EalA}v_{a}{}^{2} & \left(\left\|\mathbf{v}_{a}\right\| - l_0\right) & 0 \end{bmatrix}^{T} \tag{12} $$

where l_0 is spring original length. The spring actual space lies in the *principal central axes of elasticity*. The spring is sometimes called as the *elastic insulator*. There is considered a radi-axial spring which is able to transfer radial Q_1 and axial force Q_3. The action radial force is sometimes called bending force (Ponomarev).

4.3. Damper element

The l-th damper element is an energy dissipator with almoust 0% energy accumulation and causes a force effect between the a-th and the b-th body in the actual space *Eal*

$$ {}^{a}\mathbf{Q}_{Eal}\left({}^{a0}\dot{\mathbf{q}}_{a},\ {}^{b0}\dot{\mathbf{q}}_{b}\right) = \left[\begin{array}{cccc|cccc} 0 & 0 & Q_3(v) & 0 & 0 & 0 & 0 & 0 \end{array}\right]^{T} \tag{13} $$

where v is damper axial velocity, the damper end point in the a-th body space is ${}^{a}\mathbf{r}_{B} = {}^{a}\mathbf{T}_{b}\left({}^{a0}\mathbf{q}_{a},\ {}^{b0}\mathbf{q}_{b}\right){}^{b}\mathbf{r}_{B}$.

4.4. Contact creep element

4.4.1. Constrains

The wheel set is constrained by the rails which takes away three degrees of freedom. The wheel set can move in the longitudinal, lateral and vertical spin direction. The contact conditions of the rails and wheel set at the time t are

$$\begin{aligned} {}^{g}\mathbf{r}_{r1}(t) - {}^{g}\mathbf{r}_{w1}(t) &= \mathbf{0}, & {}^{g}\mathbf{n}_{r1}(t) + {}^{g}\mathbf{n}_{w1}(t) &= \mathbf{0}, \\ {}^{g}\mathbf{r}_{r2}(t) - {}^{g}\mathbf{r}_{w2}(t) &= \mathbf{0}, & {}^{g}\mathbf{n}_{r2}(t) + {}^{g}\mathbf{n}_{w2}(t) &= \mathbf{0} \end{aligned} \tag{14}$$

where ${}^{g}\mathbf{n}_{rj}(t)$, ${}^{g}\mathbf{n}_{wj}(t)$ is a normal vector of the *j*-th rail, wheel. This system of 12 nonlinear equations $\mathbf{F}(\mathbf{x}(t)) = \mathbf{0}$ solves the unknow vector

$$\mathbf{x}(t) = \left[u_{r1}{}^{1} \quad u_{r1}{}^{2} \quad u_{w1}{}^{1} \quad u_{w1}{}^{2} \mid u_{r2}{}^{1} \quad u_{r2}{}^{2} \quad u_{w2}{}^{1} \quad u_{w2}{}^{2} \mid z \quad \phi \right]^{T} \in \mathbb{R}^{10} \tag{15}$$

hence two equations of the system equations, Eq. 14, can be omited. Then the *m*-th axle shaft coordinate and velocity is

$${}^{m0}\mathbf{q}_{m}(t) = \left[{}^{m0}r_{m}{}^{1} \quad {}^{m0}r_{m}{}^{2} \quad z \quad 1 \mid \phi \quad 0 \quad {}^{m0}\varphi_{m}{}^{3} \quad 0 \right]^{T}, \tag{16}$$

The contact creep element spaces on the rail and wheel in the wheel space *m* are designed as

$${}^{m}\mathbf{T}_{CR} = \left[{}^{m}\mathbf{t}_{r1} \quad {}^{m}\mathbf{t}_{r2} \quad {}^{m}\mathbf{n}_{r} \quad {}^{m}\mathbf{r}_{r} \right], \qquad {}^{m}\mathbf{T}_{CW} = \left[{}^{m}\mathbf{t}_{w1} \quad {}^{m}\mathbf{t}_{w2} \quad {}^{m}\mathbf{n}_{w} \quad {}^{m}\mathbf{r}_{w} \right]. \tag{17}$$

4.4.2. Constrains reactions

Let the *m*-th wheel-axle set is considered as one body. The reactions between wheels and rails are given by the condition of the static equilibrium

$${}^{m}\mathbf{Q}_{Gm} + {}^{m}\mathbf{Q}_{EmA}^{S,D} + {}^{m}\mathbf{Q}_{ErB}^{C} = \mathbf{0}_{8\times 1}, \qquad {}^{m}\mathbf{Q}_{ErB}^{C} = \left[{}^{m}\mathbf{\Pi}_{Er1B} \quad {}^{m}\mathbf{\Pi}_{Er2B} \right] \begin{bmatrix} {}^{Er1B}\mathbf{Q} \\ {}^{Er2B}\mathbf{Q} \end{bmatrix} \tag{18}$$

where the reactive force effect at the contact element has the form ${}^{ErlB}\mathbf{Q}^{C} = \left[0 \quad 0 \quad {}^{ErlB}F^{3} \quad 0 \mid 0 \quad 0 \quad 0 \quad 0 \right]^{T}$. The force effect

$${}^{m}\mathbf{Q}_{Gm} + {}^{m}\mathbf{Q}_{ErB}^{C} = \bar{\mathbf{Q}} \tag{19}$$

is frequently called the gravitational stiffness, hence *longitudinal*, *lateral* and *yaw* respectively, the normal force ${}^{ErlB}F^{3}$, Eq. 18, in the *l*-th contact creep element is called the *wheel force.*

4.4.3. Creep force effect

4.4.3.1. Wheel-rail contact surface

Let two bodies with different materials are pressed together. Then, according to the Hertz's theory, the shape of the contact region has an elliptical boundary. The semiaxes a_1 and a_2 of such contact ellipse in the longitudinal and lateral directions are given

$a_j = m_j \left[\dfrac{3\pi N (K_1 + K_2)}{4K_3} \right]^{\frac{1}{3}}$ where the auxiliary function $m_j(\theta)$, $j \in \{1, 2\}$ (m_1 is marked as *m* and m_2 is marked as *n* in the Hertz's theory) is a function of $\theta = \operatorname{acos}\left(\dfrac{K_4}{K_3} \right) \dfrac{180}{\pi}$ [°] where functions K_k, $k \in \{1, \ldots, 4\}$, are defined

$$K_k = \frac{1-\nu_i^2}{\pi E_i},\ k \in \{1, 2\},\ K_3 = \frac{1}{2}\sum_{i=1}^{2}\sum_{j=1}^{2}\kappa_{ij},\ K_4 = \frac{1}{2}\left[\sum_{i=1}^{2}\left(\kappa_{i1} - \kappa_{i2}\right)^2 + 2\cos(2\alpha)\prod_{i=1}^{2}\left(\kappa_{i1} - \kappa_{i2}\right) \right]^{\frac{1}{2}} \tag{20}$$

where κ_{ij} is a principal curvature of the i-th contact body in the j-th direction (longitudinal direction for $j = 1$ and lateral direction for $j = 2$, rail $i = 1$, wheel $i = 2$), angle α (marked as ψ in the Hertz's theory) is between normal planes that contain the principal curvatures κ_{11} and κ_{21}, N is a reactive total normal force affecting the wheel. The radius of curvature of a body is considered to be positive if the corresponding center of curvature is within the body.

4.4.3.2. Creep force effect

The creep force effect at the contact creep element is described by the Kalker's linear theory of a rolling contact, Kalker (1967),

$$ {}^{Eil}\mathbf{Q}^{C}_{Eil} = -\mathbf{C}(\mathbf{q})\ \mathbf{g}(\mathbf{q},\dot{\mathbf{q}}) \tag{21}$$

where $\mathbf{C}$ is a square antisymetrical matrix function and $\mathbf{g}$ is a creepages vector function between contacting bodies. This Eq. 21 has the form

$$ {}^{Eil}\mathbf{Q}^{C}_{Eil} = \begin{bmatrix} T_x \\ T_y \\ 0 \\ 0 \\ 0 \\ 0 \\ M_z \\ 0 \end{bmatrix} = \left[\begin{array}{cccccccc} (a_1a_2)^1 GC_{11} & 0 & 0 & 0 & 0 & 0 & 0 & 0 \\ & (a_1a_2)^1 GC_{22} & 0 & 0 & 0 & 0 & (a_1a_2)^{1,5} GC_{27} & 0 \\ & & 0 & 0 & 0 & 0 & 0 & 0 \\ & & & 0 & 0 & 0 & 0 & 0 \\ \hline & & & & 0 & 0 & 0 & 0 \\ & & & & & 0 & 0 & 0 \\ & & & & & & (a_1a_2)^2 GC_{77} & 0 \\ -sym & & & & & & & 0 \end{array}\right] \begin{bmatrix} \gamma_1 \\ \gamma_2 \\ 0 \\ 0 \\ 0 \\ 0 \\ \gamma_7 \\ 0 \end{bmatrix} \tag{22}$$

where T_x, T_y, M_z is longitudinal, lateral and spin creep force effect respectively. The Kalker's theory proposed the so called *combined elastic constants* G, ν, that can be used as an approximation for the case of two rolling bodies with different elastic constants in determining the creepage functions C_{ij}. Then G and ν are given by

$$ \frac{1}{G} = \frac{1}{2}\sum_{i=1}^{2}\frac{1}{G_i} \quad \Rightarrow \quad G = \frac{2G_1G_2}{G_1+G_2}, \qquad \frac{\nu}{G} = \frac{1}{2}\sum_{i=1}^{2}\frac{\nu_i}{G_i} \quad \Rightarrow \quad \nu = \frac{GG_1\nu_2 + GG_2\nu_2}{2G_1G_2} \tag{23}$$

where G_i, ν_i are shear modulus of rigidity and the Poisson's ratio of the i-th body material, G, ν are combined material constants. For G_i holds true relationship $G_i = \dfrac{E_i}{2(1+\nu_i)}$ where E_i is the Young's modul of rigidity at pull. The Kalker's creep function $C_{ij} = C_{ij}\left(\dfrac{a_1}{a_2},\ \nu\right)$ depends on the ratio a_1/a_2 of the semiaxes of the contact elliptical surface and the Poisson's ratio ν. These Kalker's continuous creep functions C_{ij} are obtained from a discrete creep functions, Garg, Dukkipati (1984), by the cubic spline interpolation method.

4.4.3.3. Creepages determination

Creepage occurs in all three directions in which a relative motion can occur. This creepage or relative slip at the contact point of the i-th wheel set and the j-th wheel in the k-th direction is defined as a quotient of the slide velocity in this direction and the forward velocity v of a ve-

hicle generally ${}^{Eil}\gamma_k = \frac{v_{slide,k}}{|v|}$. It is obtained the creepage in the longitudinal γ_1, the lateral γ_2 and the normal γ_7 direction, Siegl , Švígler (2006).

4.4.3.4. Tangential creep force modification

The equations of Johnson and Vermeulen (1964) then modify the tangential forces because of creep force linearization, when the tangential force size can exceed the friction force which is unreal. The friction force is expressed fN where f is a static dry friction coefficient between the rail and the wheel. The equations of Johnson and Vermeulen then modify the tangential forces as follows $\bar{T}_i = \frac{\bar{T}}{T} T_i$ where $T = \sqrt{T_x^2 + T_y^2}$ is the total size of tangential force, $\bar{T} = fN\left[\frac{1}{1}\left(\frac{T}{fN}\right)^1 - \frac{1}{3}\left(\frac{T}{fN}\right)^2 + \frac{1}{27}\left(\frac{T}{fN}\right)^3\right]$ for $T \le 3fN$, $\bar{T} = fN$ for $T > 3fN$ and $N = \left\| F_{ErlB}{}^3 \right\|$.

4.5. Wheel–rail common parameters

The distance of the default wheel contact circles is l = 1 500 [*mm*], the wheel conicity is $\lambda = 1/40$ [1] and the static dry friction coefficient between the rail and the wheel is considered for $f_{RW} = 0{,}4$ [1].

4.6. Railway

A railway consist of two direct unwaved and waved segment, Fig. 2.

4.6.1. Rail

The rail, i = 10, has material parameters $m_i = \infty$ [*kg*], ${}^{i}\mathbf{I}_i = \mathrm{diag}([\infty \quad \infty \quad \infty])$ $[kgm^2]$, the Young's rigidity modulus at pull E_i = 210 [*GPa*] and the Poisson's ratio v_i = 0,25 [1]. The rail head part is considered only. The *j*-th rail boundary, ergo surface, is described by continuous matrix function determining the field of local spaces in the global space *g*

$$
\begin{gathered}
{}^{g}\mathbf{T}_{ij}\left(\mathbf{u}_{4j}\right) = {}^{g}\mathbf{T}_{D1}\underbrace{{}^{D1}\mathbf{T}_{C1k}\left(t_1\left(u_{ij}{}^{1}\right)\right)}_{\text{Railway center line}}{}^{C1}\mathbf{T}_{Rj}\,{}^{Rj}\mathbf{T}_{D2\,jk}\left(t_1\left(u_{ij}{}^{1}\right)\right)\underbrace{{}^{D2\,jk}\mathbf{T}_{C2k}\left(t_2\left(u_{ij}{}^{2}\right)\right)}_{\text{Rail profile}}, \\
\mathbf{u}_{ij} = \left[u_{ij}{}^{1} \quad u_{ij}{}^{2}\right]^T \in \Omega \subset \mathbb{R}^2,\ \Omega = \langle 0,2\rangle \times \langle -4,4\rangle
\end{gathered}
\tag{24}
$$

where the first rail surface parameter $u_{ij}{}^{1}$ determines position in the railway direction, the second $u_{ij}{}^{2}$ determines position on the rail profile, the curve number and the local coordinate t_D in the *D*-th direction are given by $k = 1 + \mathrm{fix}\left(u_{ij}{}^{D}\right)$, $t_D = u_{ij}{}^{D} - \mathrm{fix}\left(u_{ij}{}^{D}\right)$. The space of the *j*-th rail *Rj* is defined

$${}^{C1k}\mathbf{T}_{Rj} = \mathbf{T}_2\left(\left(-1\right)^{(j-1)}\frac{l}{2}\right)\mathbf{T}_4\left(\left(-1\right)^{(j-1)}\mathrm{atan}\left(\lambda\right)\right). \tag{25}$$

The space *Dd* defines a position of the composite curve *Cd* in the *d*-th direction, ${}^{g}\mathbf{T}_{D1} = \mathbf{T}\left({}^{g}\mathbf{q}_{D1}\right)$, ${}^{Rj}\mathbf{T}_{D2\,jk} = \mathbf{T}\left(\mathbf{q}_{D2\,jk}\left(t_1\left(u_{ij}{}^{1}\right)\right)\right)$. The coordinates $\mathbf{q}_{D2\,jk}$ are designed

$$\mathbf{q}_{D2\,j1}\left(t_{11max}t_1\right)=\mathbf{0}_{8\times1},$$

$$\mathbf{q}_{D2\,j2}\left(t_{12max}t_1\right)=\left[\begin{array}{cc|c|cc|cc}0 & 0 & A_j\left[\cos\left(\frac{2\pi}{L_j}t_{12max}t_1\right)-1\right] & 1 & 0 & -\operatorname{atan}\left[-A_j\sin\left(\frac{2\pi}{L_j}t_{12max}t_1\right)\frac{2\pi}{L_j}\right] & 0 & 0\end{array}\right]^T. \tag{26}$$

The curve *Cdk* is defined in the fix space *Pdk* by the vector function

$${}^{Dd}\mathbf{r}_{Cdk}\left(t_d\left(u_{ij}{}^d\right)\right)={}^{Dd}\mathbf{T}_{Pdk}\,{}^{Pdk}\mathbf{T}_{Adk}\left(t_{dkmax}t_d\right)\left[R_{dk}\quad 0\quad 0\quad 1\right]^T. \tag{27}$$

The fix spaces *Pdk* for the railway curve are defined

$$\begin{aligned}{}^{D1}\mathbf{T}_{P11}&=\mathbf{E}_{4\times4},\\ {}^{D1}\mathbf{T}_{P12}&={}^{D1}\mathbf{T}_{P11}\,{}^{P11}\mathbf{T}_{C11}\left(t_{11max}\right),\\ {}^{D1}\mathbf{T}_{P13}&={}^{D1}\mathbf{T}_{P12}\,{}^{P12}\mathbf{T}_{C12}\left(t_{12max}\right)\mathbf{T}_6\left(\pi/2\right)\mathbf{T}_1\left(R_{13}\right)\mathbf{T}_4\left(\pi\right).\end{aligned} \tag{28}$$

The rail profile is modeled in accordance with the profile UIC 60. The matrices of geometrical parameters are

$$\mathbf{P}_{rd}=\begin{bmatrix}t_{dkmax}\\ R_{dk}\end{bmatrix},\quad \mathbf{P}_{r1}=\begin{bmatrix}4\,000 & 1\,000\,000\\ 0 & 0\end{bmatrix},\quad \mathbf{P}_{r2}=\begin{bmatrix}\operatorname{asin}\left(\frac{10{,}5}{300}\right) & t_{22max} & t_{23max} & t_{24max}\\ 300 & 80 & 13 & 0\end{bmatrix},$$ aplitudes

$\mathbf{A}=\left[A_1\quad A_2\right]^T$ and wave lengths $\mathbf{L}=\left[L_1\quad L_2\right]^T$.

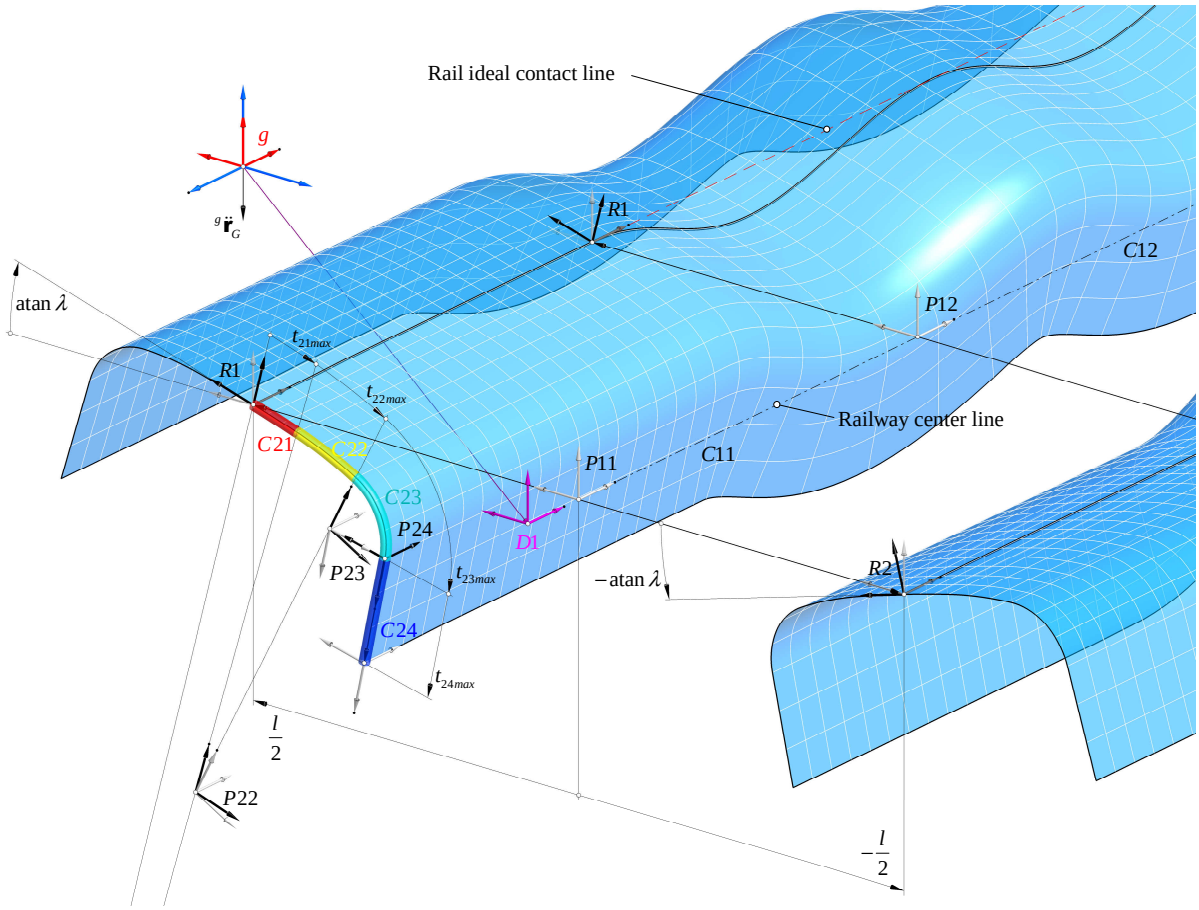

Fig. 2 Railway definition with rail profile UIC 60

4.7. Vehicle

4.7.1. Case of vehicle

To the case of vehicle, i = 1, there is added a mass of the revolving pin and upper part of the secondary suspension. The weight of these parts is in total 523 [kg]. The case mass per one vehicle bogie is considered half $m_i = \frac{1}{2}55\ 526\ [kg]$, the mass inertia tensor is considered original ${}^{i}\mathbf{I}_i = \mathrm{diag}\left([104\ 772 \quad 1\ 037\ 305 \quad 1\ 037\ 091]\right)\ [kgm^2]$ and the coordinates matrix of the vehicle bogies in the equilibrium position is ${}^{i0}\bar{\mathbf{q}}_{r0} = \left[{}^{i0}\mathbf{q}_{210}\right] = [0 \quad 0 \quad -1\ 057{,}5 \quad 1 \mid 0 \quad 0 \quad 0 \quad 0]^T$.

4.7.2. Frame of bogie

The frame of bogie, i = 2, contains own frame, brakes, sand blasting machine, wheel flange lubrication, cleaning cylinder, pipeline, cables, one half of springs and dampers, antennas and pins. The weight is m_i = 3 478 [kg], ${}^{i}\mathbf{I}_i = \mathrm{diag}\left([2\ 959 \quad 4\ 006 \quad 6\ 490]\right)\ [kgm^2]$, the coordinates matrix of the axle shafts in the equilibrium positions is

$${}^{i0}\bar{\mathbf{q}}_{r0} = \left[{}^{i0}\mathbf{q}_{310} \quad {}^{i0}\mathbf{q}_{320}\right] = \left[\begin{array}{cccc|cccc} 1\ 250 & 0 & -164{,}634 & 1 & 0 & 0 & 0 & 0 \\ -1\ 250 & 0 & -164{,}634 & 1 & 0 & 0 & \pi & 0 \end{array}\right]^T,$$

the coordinates matrix of the link element spaces *EilA* on the frame left side is

Springs		*Dampers*		
		Longitudinal	*Lateral*	*Vertical*
170	−170	−400	590	405
1 370	1 370	1 460	1 060	1 382
−165	−165	−121	47,5	−182
1	1	1	1	1
0	0	0	$-\left(\frac{\pi}{2} - 8\frac{\pi}{180}\right)$	0
0	0	$-\left(\frac{\pi}{2} - 8\frac{\pi}{180}\right)$	0	0
0	0	0	0	0
0	0	0	0	0

$$ {}^{i}\bar{\mathbf{q}}_{EiA} = \left[{}^{i}\mathbf{q}_{EilA}\right] = \quad , \qquad (29)$$

on the right side they are rotated by π arround the vertical axis and added to this matrix.

4.7.3. Axle shaft

The axle shaft, i = 3, contains own axle shaft only. The weight is m_i = 840,8 [kg], ${}^{i}\mathbf{I}_i = \mathrm{diag}\left([156{,}5 \quad 68{,}8 \quad 156{,}5]\right)\ [kgm^2]$, the coordinates matrix of the connecting bodies is

$${}^{i0}\bar{\mathbf{q}}_{r0} = \left[{}^{i0}\mathbf{q}_{40} \quad {}^{i0}\mathbf{q}_{50} \quad {}^{i0}\mathbf{q}_{610} \quad {}^{i0}\mathbf{q}_{620}\right] = \left[\begin{array}{cccc|cccc} 0 & 1\ 109{,}5 & 47 & 1 & 0 & 0 & 0 & 0 \\ 0 & -1\ 109{,}5 & 47 & 1 & 0 & 0 & 0 & 0 \\ \hline 0 & l/2 & 0 & 1 & 0 & 0 & 0 & 0 \\ 0 & -l/2 & 0 & 1 & 0 & 0 & \pi & 0 \end{array}\right]^T.$$

The axle shaft is fixle connected with the wheels and axle boxes. This connection is modeled by fixed link

element. Then motion of these fixly connected parts is dependent on the shaft kinematical magnitudes ${}^{i0}\mathbf{q}_i$, ${}^{i0}\dot{\mathbf{q}}_i$ ${}^{i0}\ddot{\mathbf{q}}_i$.

4.7.4. Axle box left

The axle box, i = 4, contains bearing housing, roll bearings, sealing labyrinths, Earth return brush, anti-wheel slide control, bearing housing cover, half of primary springs and dampers, pin of the connecting rod and half of rubber-metal vibration damper of the connecting rod. The mass of this assembly is $m_i = 232\ [kg]$, ${}^{i}\mathbf{I}_i = \mathrm{diag}([6{,}2 \quad 12{,}8 \quad 14{,}3])\ [kgm^2]$, the coordinates matrix of the link element spaces *EilA* is

$$ {}^{i}\bar{\mathbf{q}}_{EiA} = \left[{}^{i}\mathbf{q}_{EilA} \right] = \begin{array}{c} \begin{array}{cccc} \textit{Springs} & & \textit{Connecting rod} & \textit{Damper vertical} \end{array} \\ \left[\begin{array}{cc|c|c} 310 & -270 & -398 & -270 \\ -49{,}5 & -49{,}5 & -49{,}5 & 155 \\ 78 & 78 & -76 & -122 \\ 1 & 1 & 1 & 1 \\ \hline 0 & 0 & 0 & 0 \\ 0 & 0 & -\frac{\pi}{2} & 0 \\ 0 & 0 & 0 & 0 \\ 0 & 0 & 0 & 0 \end{array}\right] \end{array} . \tag{30} $$

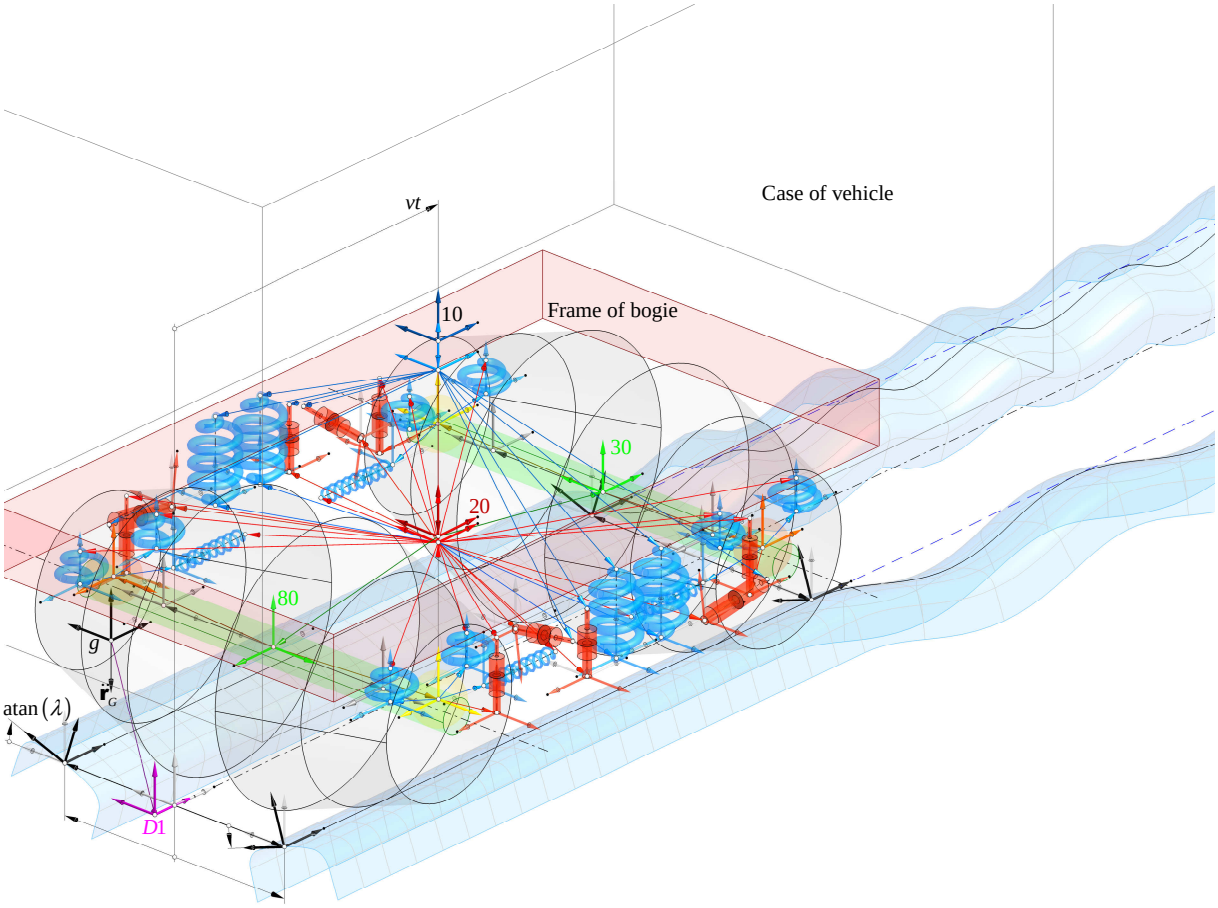

Fig. 3 Railway vehicle in the equilibrium state on the ideal railway segment

4.7.5. Axle box right

The axle box, i = 5, is the same as on the left but reflected arround the longitudinal vertical plane.

4.7.6. Wheel

The wheel, i = 6, contains own wheel, breaking discs, carrier of Earth return brush and outer flange of teeth clutch. The mass parameters are m_i = 630,6 [kg], ${}^{i}\mathbf{I}_i = \mathrm{diag}\left(\left[185{,}5 \quad 137{,}6 \quad 185{,}5\right]\right)$ $\left[kgm^2\right]$, the Young's rigidity modulus at pull E_i = 210 [GPa], the Poisson's ratio v_i = 0,25 [1], the contact circle D = 1 250 [mm] and the wheel width w = 150 [mm]. The wheel rolling surface is considered as a conical surface which is described by vector function in the mass centre space i

$$ {}^{i}\mathbf{r}_i\left(\mathbf{u}_i\right) = \mathbf{T}_5\left(u_i^{\,2}\right)\left[\frac{D}{2} - \lambda u_i^{\,1} \quad u_i^{\,1} \quad 0 \quad 1\right]^T, \quad \mathbf{u}_i = \begin{bmatrix} u_i^{\,1} \\ u_i^{\,2} \end{bmatrix} \in \Omega \subset \mathbb{R}^2, \quad \Omega = \left\langle -\frac{w}{2},\ \frac{w}{2} \right\rangle \times \langle 0,\ 2\pi \rangle \quad (31) $$

where u^k are curvilinear coordinates on the wheel surface, resp. coordinates on the profile and circumference. The local spaces field on the wheel surface is

$$ {}^{i}\mathbf{T}_i\left(\mathbf{u}_i\right) = \left[{}^{i}\mathbf{t}_{i1} \quad {}^{i}\mathbf{t}_{i2} \quad {}^{i}\mathbf{n}_i \quad {}^{i}\mathbf{r}_i \right] \quad (32) $$

where tangential and normal vectors at each wheel point are

$$ {}^{i}\mathbf{t}_{id}\left(\mathbf{u}_i\right) = \frac{\partial\, {}^{i}\mathbf{r}_i}{\partial u_i^{\,d}}, \qquad {}^{i}\mathbf{n}_i\left(\mathbf{u}_i\right) = \mathrm{v2m}\left({}^{i}\mathbf{t}_{i1} \right) {}^{i}\mathbf{t}_{i2}. \quad (33) $$

The local spaces field on the wheel surface at the global space g is ${}^{g}\mathbf{T}_i\left(\mathbf{u}_i\right) = {}^{g}\mathbf{T}_i\, {}^{i}\mathbf{T}_i\left(\mathbf{u}_i\right)$. The wheel is linked by the contact creep element C whose actual space ${}^{i}\mathbf{T}_C$ is given by the Eq. 17.

4.7.7. Link elements

All springs and dampers are produced by KONI company. All the element characteristics are given by discrete functions which are interpolated to the continuous functions by *spline* or *piecewise cubic Hermite* approximation methods. The second interpolation method has no overshoots and less oscillation if a data are not smooth. The element force functions are shown in the following figures where white points and red curve represents a discrete and continuous force functions in eigen space *Eil*. However, radial or bending force of a spring is described in the original space *Eil*0. The force and damping functions are ploted in red and blue color on the Fig. 4 up to 7. The yaw damper is specially designed to control small-amplitude sinusoidal bogie rotational movements and thereby enable trains to be operated at speeds above those previously possible.

4.7.7.1. Spring primary

The length of free spiral spring is 219,4 [mm], pitch diameter 250 [mm], diameter of the wire 44 [mm]. The stiffnesses in the origin are in the radial direction 2 366 [Nmm^{-1}] and in the axial direction 1 177 [Nmm^{-1}]. The spring has 2 effective threads.

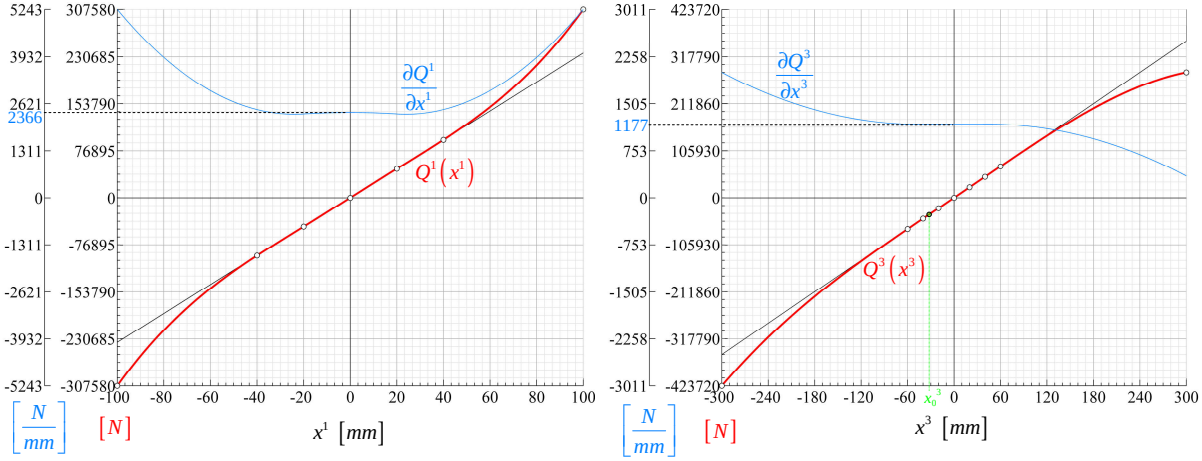

Fig. 4 Spring primary – radial and axial force

4.7.7.2. Spring secondary

The length of free spiral spring is 630 [*mm*], pitch diameter 240 [*mm*], diameter of the wire 48 [*mm*]. The stiffnesses in the origin are in the radial direction 266 [Nmm^{-1}] and in the axial direction 538 [Nmm^{-1}]. Number of spring effective threads is 7.

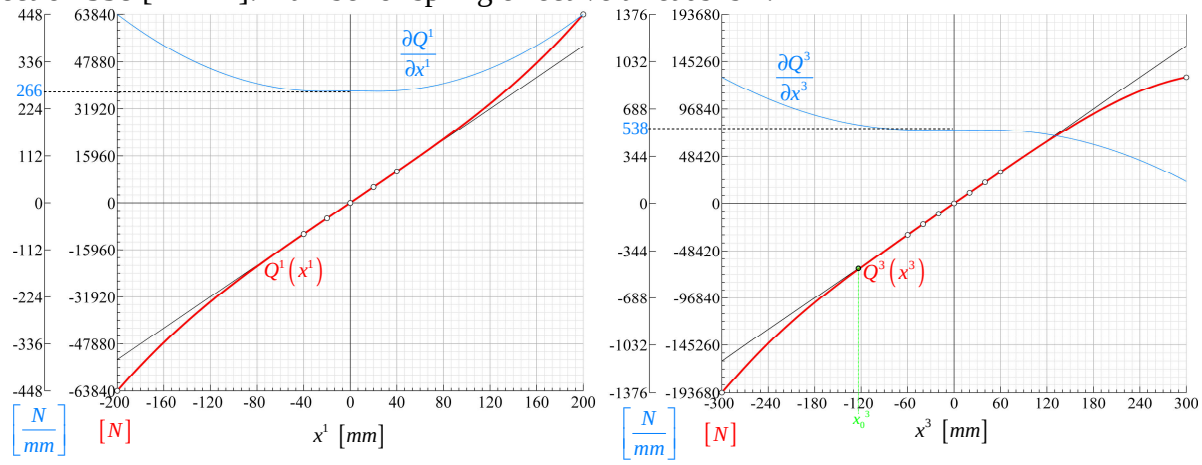

Fig. 5 Spring secondary – radial and axial force

4.7.7.3. Connecting rod axle box – frame

The stiffness of the connecting rod is considered for parameters E = 210 [*GPa*], D = 42 [*mm*], l_0 = 545 [*mm*] in this way

$$k = \frac{EA}{l_0} = \frac{E\pi D^2}{4l_0} \cong 533\,840 \left[\frac{N}{mm}\right]. \tag{34}$$

4.7.7.4. Dampers

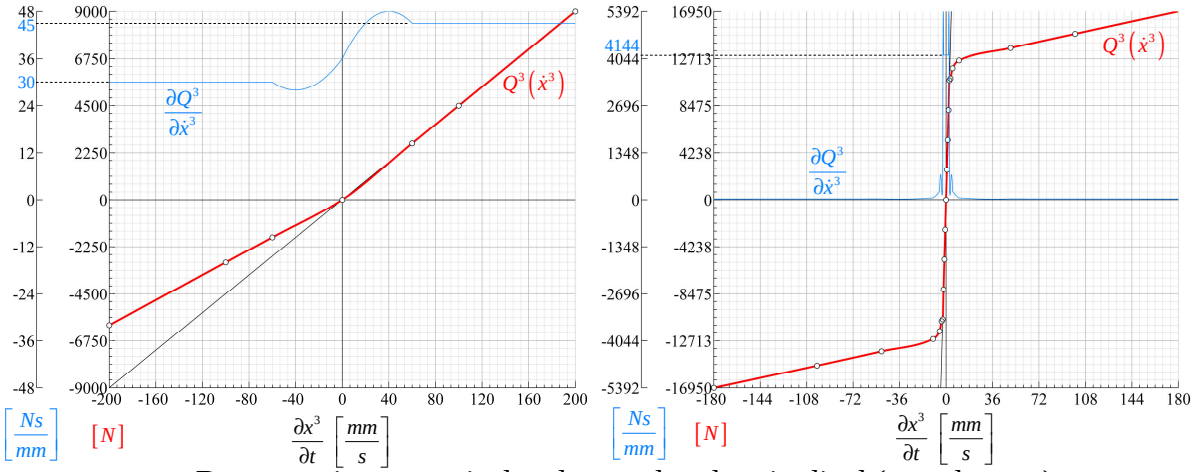

Fig. 6 Damper primary vertical and secondary longitudinal (yaw damper)

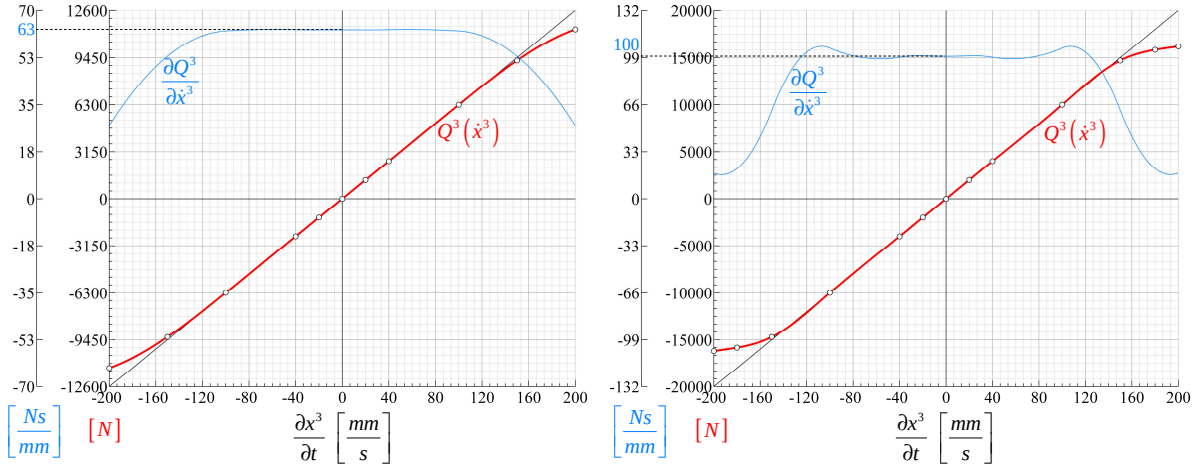

Fig. 7 Damper secondary lateral and secondary vertical

5. Model construction

5.1. Vehicle building

The moving space is placed into the case equilibrium space 10, see Eq. 9. Because the multi-body system of the vehicle has a *finite tree structure* there is created a builder with the *recursive* algorithm of a whole vehicle system. A list of the bodies is shown in the Tab. 2.

Absolute number m	Name	Description	Part i	Copy j	Tree level L	${}^{m0}\mathbf{T}_{r0}$		Degrees of freedom
						m	r	
1	Case of vehicle		1	1	1	1	1	6
2	Frame of bogie	front	2	1	2	1	2	6
3	Axle shaft	front	3	1	3	2	3	3
4	Axle box left		4	1	4	3	4	1
5	Axle box right		5	1	4	3	5	1
6	Wheel	left	6	1	4	3	6	0
7	Wheel	right	6	2	4	3	7	0
8	Axle shaft	back	3	2	3	2	8	3
9	Axle box left		4	2	4	8	9	1
10	Axle box right		5	2	4	8	10	1
11	Wheel	left	6	3	4	8	11	0
12	Wheel	right	6	4	4	8	12	0

Tab. 2 Bodies list

5.2. *Motion equations*

The condition of the *m*-th body dynamical equilibrium in the actual space *m* is

$$ {}^{m}\mathbf{Q}_{m}(t) = \mathbf{0}_{8\times 1} \tag{35} $$

where the force effect on the *m*-th body is described by the Eq. 4. The Eq. 35 represents a system of ordinary second-order differential equations.

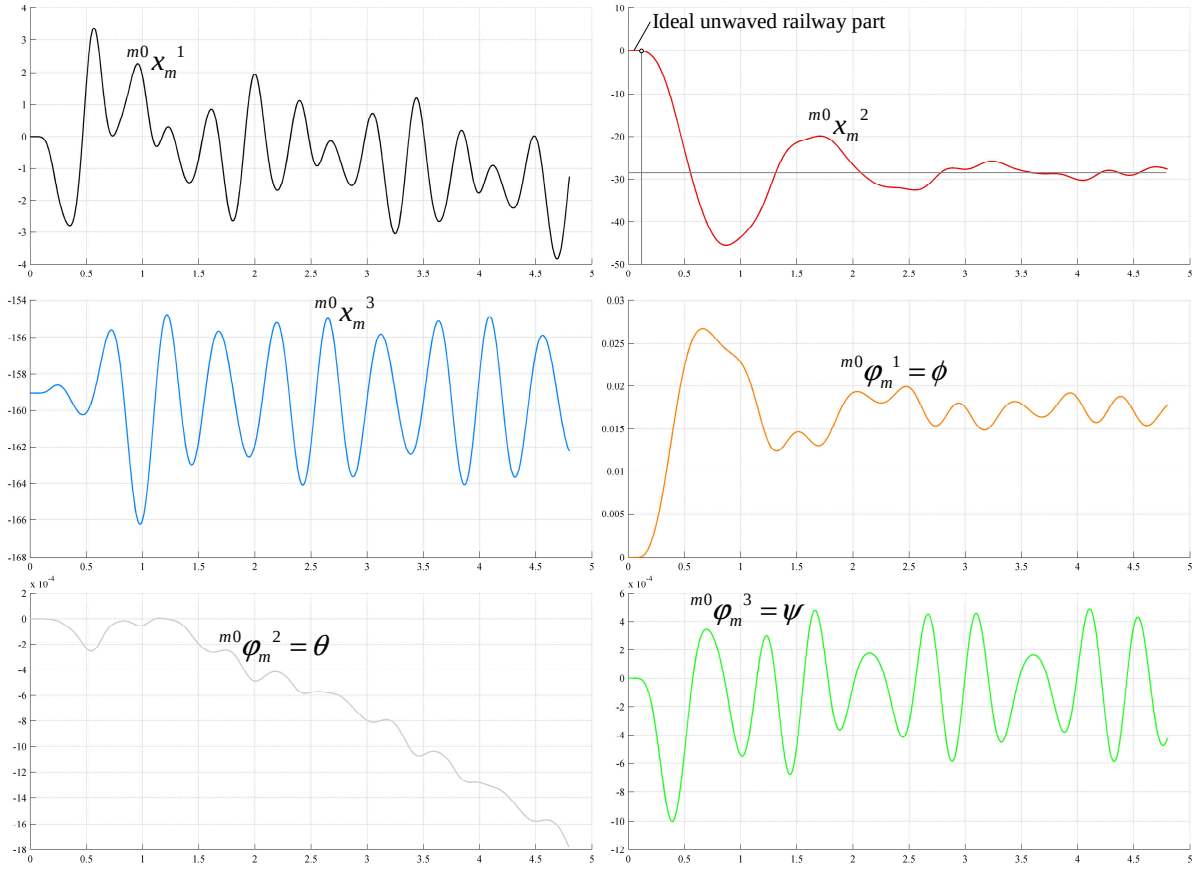

Fig. 8 Coordinates of the case motion, *m* = 1

6. Numerical simulation

For reasons of large-scale numerical calculations the authors decided to verify given complex mathematical with simplifications. This simplifications are made by zero mass of the front and the back wheel-axle sets which are assembled from shaft, wheels and axle boxes. This final multibody system has consequently 12 degrees of freedom. The numerical simulation is made for initial values $\mathbf{q}_0 = \left[{}^{10}\mathbf{q}_{10}{}^{T} \quad {}^{20}\mathbf{q}_{20}{}^{T} \mid {}^{10}\dot{\mathbf{q}}_{1}{}^{T} \quad {}^{20}\dot{\mathbf{q}}_{2}{}^{T} \right]^{T} = \mathbf{0}_{24\times 1}$, ${}^{10}q_{10}{}^{3} \cong -159{,}05\ [mm]$, ${}^{20}q_{20}{}^{3} \cong -32{,}54\ [mm]$ and forward velocity v = 60 [kmh^{-1}]. The waviness of the second direct railway segment is considered with amplitudes $\mathbf{A} = [-12 \quad 12]^{T}\ [mm]$ and with wave lengths $\mathbf{L} = [6 \quad 10]^{T}\ [m]$ for the left and right rail respectively. The negative amplitude A_1 means the left rail oscillates above ideal rail and therefore the vehicle bodies has positive roll angle. Coordinates, ${}^{m0}q_{m}{}^{i}(t)\ [mm]$, of the case, the frame and the front wheel-axle set are plotted in the time dependence in seconds in the Fig. 8 up to 10. The coordinate

${}^{m0}\mathbf{q}_m = \left[{}^{m0}x_m{}^1 \quad {}^{m0}x_m{}^2 \quad {}^{m0}x_m{}^3 \quad 1 \,\middle|\, {}^{m0}\varphi_m{}^1 \quad {}^{m0}\varphi_m{}^2 \quad {}^{m0}\varphi_m{}^3 \quad 0 \right]^T$ indicates position of the *m*-th body in the equilibrium space *m*0. This railway wavines type causes the vehicle case lateral displacement approximately up to –29 [*mm*], see ${}^{10}x_1{}^2(t)$ and frame lateral displacement approximately up to –3,6 [*mm*], see ${}^{20}x_2{}^2(t)$. The vehicle motion on the ideal railway should not be theoretically but for reason numerical inaccuracy and the time discretication the small motion randomly can occur.

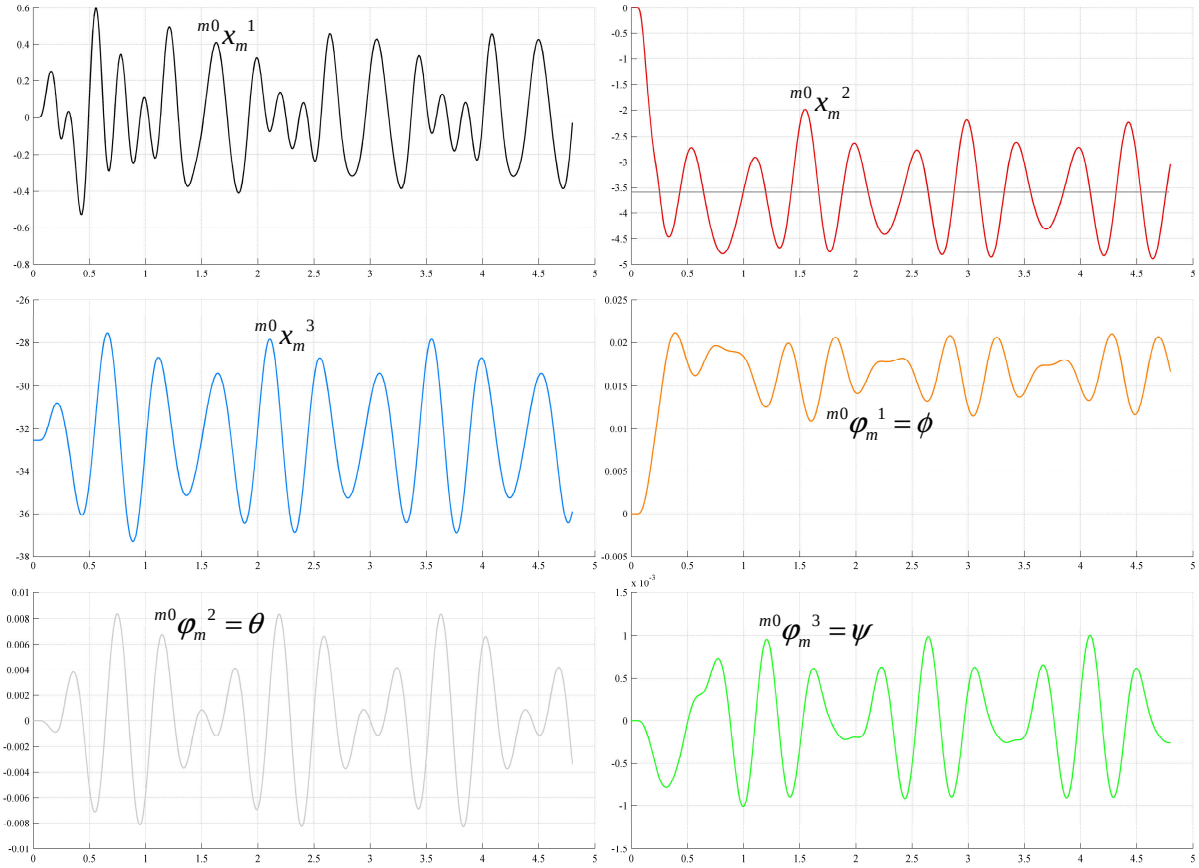

Fig. 9 Coordinates of the frame motion, *m* = 2

7. Conclusions

The mathematical model of the railway vehicle bogie and the numerical solution of the simplified mathematical model is made by own software which allows to simulate a multibody system oscillation in dependence on initial values. The next work will be oriented to the finishing of the complete numerical simulation and to the creation of mathematical model of a complete railway vehicle with two doubly suspended bogies and eventually with consideration of a finite stiffness of rail with subsoil.

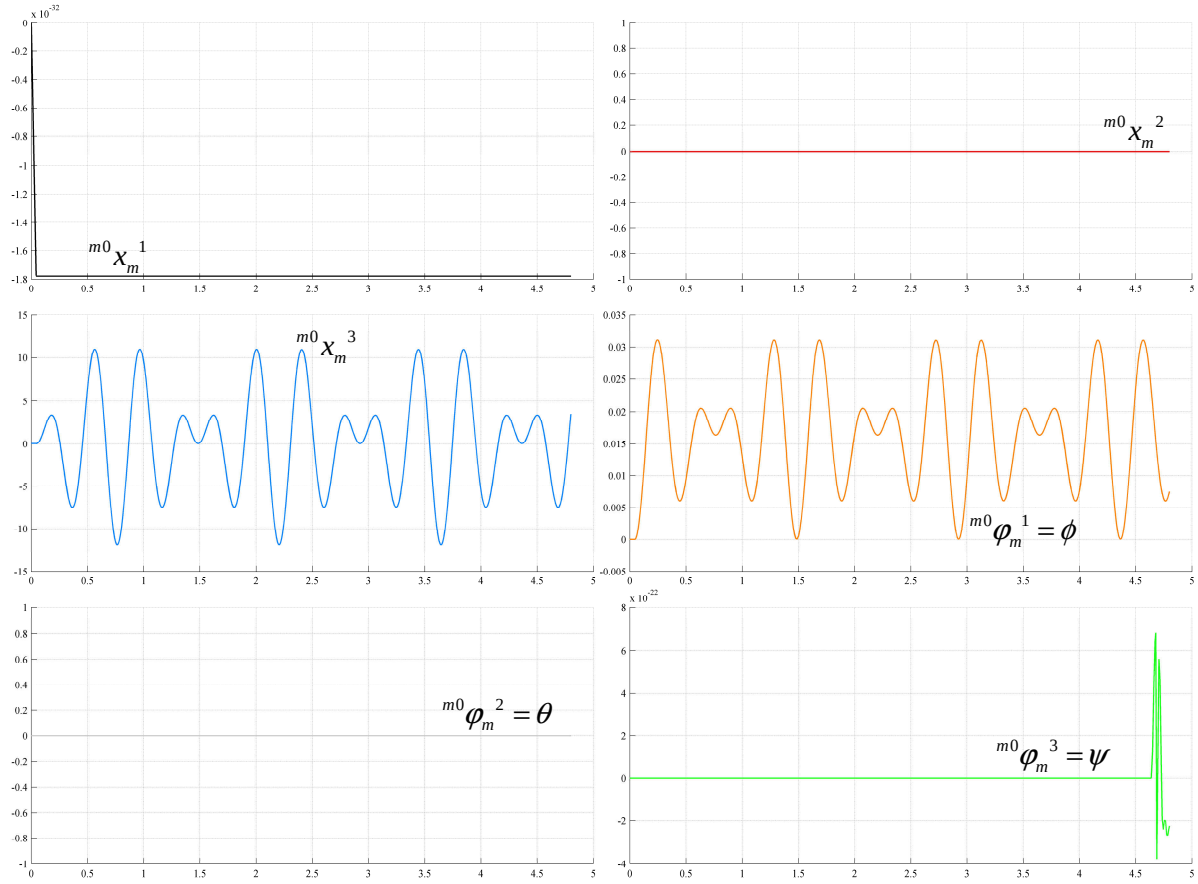

Fig. 10 Coordinates of the front axle, m = 3, with 0 degrees of freedom, vertical and roll motion is given by wheel set – rails contact

8. Acknowledgement

The paper was written with the support of the project MŠMT 1M0519 – The Research Centre of Rail Vehicles and the research project MSM 4977751303.

9. References

Garg, V. K. & Dukkipati, R. V. (1984) *Dynamics of Railway Vehicle Systems*. Academic publisher, London, Great Britain.

Kalker, J. J. (1967) *On the Rolling Contact of Two Elastic Bodies in the Presence of Dry Friction*, Ph. D. dissertation, Delft University of Technology, Delft, Netherlands.

Machulda, V., Švígler, J., Siegl, J. (2008) Modellling of contact between wheel set and uneven railway. *Computational Mechanics 2008*, Hrad Nečtiny, Czech Republic.

Siegl, J., Švígler, J. (2008) The Motion Simulation of the Railway Vehicle Bogie emphatically of Creep Force Effects. *Engineering Mechanics 2008*, Svratka, Czech Republic (full text on CD, extended abstract on pages 206 – 207).

Zeman, V., Hlaváč Z., Byrtus, M. (2008) Dynamical Analysis of the Railway Vehicle Bogie. *Engineering Mechanics 2008*, Svratka, Czech Republic (full text on CD, extended abstract on pages 284 – 285).